Experimental Study of the Stark Broadened Helium Ion Lines HeII 121.5, 164.0 and 468.6 nm

A. Piel and J. Slupek

Institut für Experimentalphysik II der Ruhr-Universität Bochum

Using a pulsed linear discharge of high purity, Stark broadened profiles of the first two Balmer lines and the Paschen-α line of HeII have been investigated. The electron density ($N_e = 5.5 \cdot 10^{22}$ m^{-3}) was measured with a coupled cavity He-Ne laser interferometer. The intensity ratio of the HeII 468.6 nm and the HeI 471.3 nm line was employed to determine the electron temperature ($T_e = 3.8$ eV). At these plasma parameters the measured ion lines are unaffected by self absorption. This enables direct comparison with existing theories. Discrepancies between experimental and theoretical line shapes are critically discussed. Fine structure effects, usually neglected in theories, turn out to be important for the Balmer-α line.

Introduction

Stark broadening of spectral lines is of great interest in the fields of plasma diagnostics. As far as plasmas of comparatively low temperatures and densities are taken into account, Stark broadened hydrogen lines turn out to be well suited for reliable electron density measurements. In fully ionized plasmas of higher temperatures and densities, Stark broadened ion lines have to be used instead. In particular, ion line broadening is the only possible method for electron density measurement in the field of laser-produced plasmas. Thus there is great interest in theoretical and experimental results regarding ion lines. According to its hydrogenic nature, singly ionized helium is the most easy to handle ion. Thus Stark broadened HeII-lines provide a good test object for understanding the broadening mechanism of ionic lines.

The presently available calculations of HeII line profiles show large deviations from each other. In the case of the HeII Paschen-α line "unified theory" calculations of Greene [1] yield significantly narrower line profiles than earlier calculations of Kepple [2]. In the latter a modified impact theory was used, which is mainly an extension of the older theory of Griem and Shen [3]. Similar discrepancies exist for the HeII Balmer lines. Whereas for the Balmer-α line more recent calculations of Greene

[4], including ion-dynamic effects, are in quite good agreement with Kepple [2], calculations of Lee [5] predict much broader profiles. The same difference between Lee's and Kepple's results exists for the HeII Balmer-β line.

There is also weak agreement among the experimental results for several HeII-lines [6 – 14]. Recent investigations of the Paschen-α line HeII 468.6 nm [6 – 9] – which often has been used routinely to measure electron densities – yield profiles that lie between the profiles of Kepple [2] and of Greene [1]. On the other hand, measurements by Jones et al. [10] are in good accordance with Kepple's predictions. Concerning the Balmer lines HeII 164.0 nm and HeII 121.5 nm, the situation is even less satisfactory. There are only few investigations [10 – 14], which show considerable deviations from each other. Older line profile measurements by Hessberg and Boetticher [11] as well as Eberhagen and Wunderlich [12] yield narrower profiles than the theory of Kepple for both lines. On the other hand, Jones et al. [10] have not found any disagreement with Kepple for the Balmer-α line. The Balmer-β profile measured by van Zandt et al. [13] turned out to be wider than Kepple's theory, and the most recent investigations of Smith and Burgess [14] yield slightly enhanced wings of Balmer-α and Balmer-β.

Experimental uncertainties accompanying these measurements may arise from three reasons. Firstly, measured Balmer-α profiles were affected by optical depth in [11] and [14], requiring crucial corrections. Secondly, at least in [13] the Balmer-β line core is influenced by hydrogen Lyman-α absorption due to

plasma impurities. Finally, except in [14] electron densities have not been measured independently. For instance, Hessberg and Boetticher [11] as well as van Zandt et al. [13] have deduced the electron density from the line shape of the HeII 468.6 nm line. As pointed out above, there are still uncertainties regarding this line, which influence the electron density measurements.

In view of these discrepancies, further experimental work is indicated. This seems to be even more important, as no direct comparison of measured Balmer line profiles with profiles calculated according to the more recent theories of Greene [4] and Lee [5] has been carried out. In this paper we present measurements of the first two Balmer lines (HeII 164.0 nm, HeII 121.5 nm) and the Paschen-α line (HeII 468.6 nm). A pulsed linear arc discharge was used as a plasma source of high purity. The discharge parameters were chosen to avoid optical depth, which is crucial for the HeII 164.0 nm line. Electron densities were independently determined with a He-Ne laser interferometer. Measured line profiles are compared with the predictions of different theories.

I. Experimental

The experimental device is similar to that described by Piel and Richter [15] for studies of neutral helium lines at low densities. However, according to the higher densities and temperatures in this experiment and to complications of vacuum-uv spectroscopy, the actually used set-up shows several specific modifications.

1. Discharge tube

The discharge tube is shown in detail in Figure 1. It is mainly composed of a fused quartz tube (750 mm long, 25 mm i.d.) containing two ring
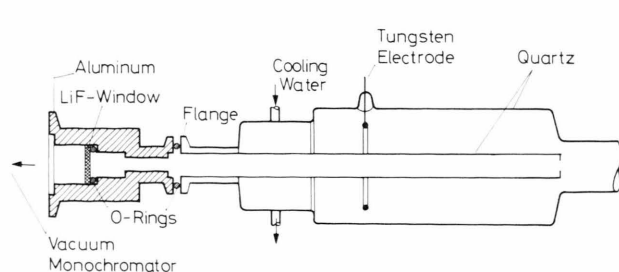
shaped tungsten electrodes at the ends. At both ends of the discharge tube the plasma light can be observed end-on through coaxial quartz tubes of smaller diameter. These tubes avoid inhomogeneous plasma areas in the vicinity of the electrodes. Observation windows are mounted in aluminum holders, which are connected with the discharge tube by water cooled flanges. The window material is quartz for observation in the visible and lithium fluoride for the vacuum-uv region. Remote mounting turned out to be necessary to protect the windows from damage by the hot plasma. A quartz rod can be inserted in order to reduce the effective plasma length on the tube axis.

By means of a heater coil the whole discharge tube can be heated to about 400 °C. Thus, as pointed out earlier by Piel and Richter [15], hydrogen impurities due to a water layer on the inner wall of the discharge tube are effectively reduced.

2. Electrical circuit

The discharge is driven by a rectangular current pulse of 350 µs duration with a peak current of several kA, generated by a high-voltage delay line (15 capacitors 7.7 µF/16 kV, 15 coils of 18 µH each). The current is switched by an externally triggered ignitron. A matching resistance R of 1.5 Ω is used for matching the discharge to the characteristic impedance of the delay line.

3. Optical arrangement

The experimental arrangement for the line profile measurements is shown in Figure 2. The plasma light is simultaneously observed end-on in the vacuum-uv and in the visible light region. In either case the plasma volume under observation is limited by a set of apertures to a cylinder of 5 mm diameter on the discharge axis.

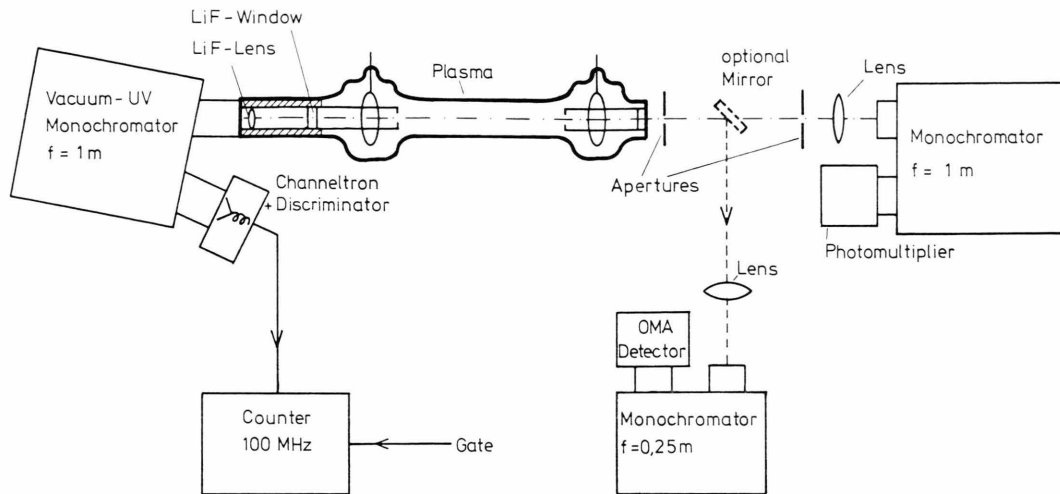Fig. 1. Discharge tube for uv spectroscopy.
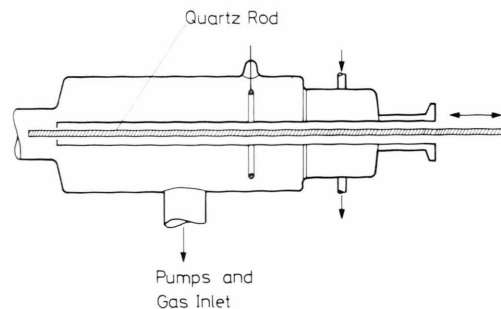
Fig. 2. Optical arrangement for simultaneous uv and visible line shape measurements.
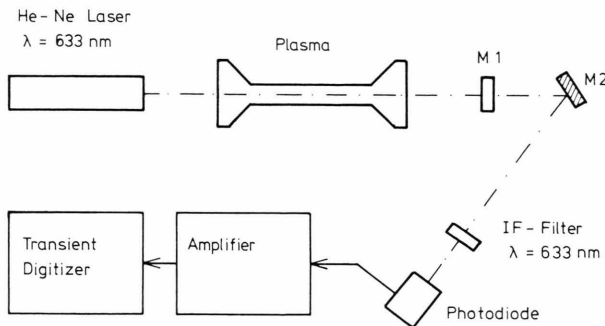

Fig. 3. Coupled cavity laser interferometer. The partially reflecting feed-back mirror M1 has a reflectivity of 80%.

Vacuum-uv spectroscopy is performed with a McPherson 225 monochromator ($f = 1$ m), equipped with a 1200 lines/mm concave grating. The plasma light is focused on the variable entrance slit by a lithium fluoride lense, which matches the solid angle of the spectrometer. A channeltron electron multiplier Bendix 4039, with a photon counting unit is used for light detection, and the uv lines are scanned shot by shot.

Two different systems are provided for visible light observation. A $f = 1$ m monochromator (1800 lines/mm grating) with a photomultiplier tube are employed for time resolved line profile measurements. Furthermore, for permanently monitoring the plasma conditions and to check the shot to shot reproducibility of the plasma, a low resolution system consisting of a $f = 1/4$ m monochromator

with OMA-system is applied. For this purpose, the HeII 468.6 nm line (Paschen-α) and neighboured HeI lines are observed simultaneously. This provides a good method for reproducibility control, since the intensity of the Paschen-α line is very sensitive to variations of the plasma temperature.

II. Diagnostic Measurements

1. Electron density

Electron density determination is performed by means of a coupled cavity laser interferometer similar to that described by Ashby and Jephcott [16]. A schematic diagram of the interferometer setup is shown in Figure 3. A standard 2 mW He-Ne laser operating at $\lambda = 633$ nm is used. After traversing the plasma twice, the laser beam reenters the laser. The feed-back mirror M1 has a reflectivity of 80%. The transmitted part of the laser light is detected by a photodiode. Disturbing plasma light is rejected by means of a narrow band interference filter. The signal is amplified and stored in a transient digitizer.

The electron density is determined from the line integrated refractivity of the plasma. Because of the low filling pressure in this discharge (typically $2 \cdot 10^3$ Pa) and the high degree of ionization on the tube axis the refractivity is entirely due to the plasma electrons. Furthermore, the plasma turned out to be sufficiently homogeneous along the tube.

Thus the electron density may be directly related to the measured interference signal, yielding an electron density change of $3.9 \cdot 10^{21}$ m^{-3} for each fringe. The measured time resolved electron density for typical discharge conditions is shown in Figure 4. Errors in the electron density determination are mainly due to the uncertainty of fixing the phase at the end of the discharge, which causes a quarter fringe error. For the conditions of Fig. 4 the accuracy can be estimated to be better than 5%. The electron density turns out to be sufficiently constant for a time interval of 100 μs around the maximum.

2. Electron temperature

The electron temperature is determined from the ratio of the HeII 468.6 nm line to the HeI 471.3 nm line, which are both optically thin in our case. Time resolved line intensities have been measured on a shot to shot basis. From a LTE model, a temperature of 3.5 ± 0.5 eV is obtained. Applying a more sophisticated collisional-radiative model according to Mewe [17] to our plasma results in a slightly higher temperature of 3.8 ± 0.5 eV. However, re-

garding the high electron density our plasma is expected to be close to LTE [18]. A higher precision is not necessary, since the electron temperature has only weak influence on the line profiles to be examined.

III. Line Profile Measurements and Results

In our discharge an electron density between 10^{22} m^{-3} and $6 \cdot 10^{22}$ m^{-3} can be achieved by variation of helium pressure and discharge current. The line profile measurements presented here have been carried out at $N_e = 5.5 \cdot 10^{22}$ m^{-3}. This choice turns out to be advantageous, since at lower densities broadening mechanisms other than Stark effect become dominant in case of the Balmer lines. At higher densities self absorption of the Balmer-α line complicates the comparison of the experimental results with theory [11, 14].

In several runs line profiles have been scanned on a shot to shot basis, averaging over ten shots for each wavelength position. The plasma was found to be sufficiently reproducible, with less than 15%
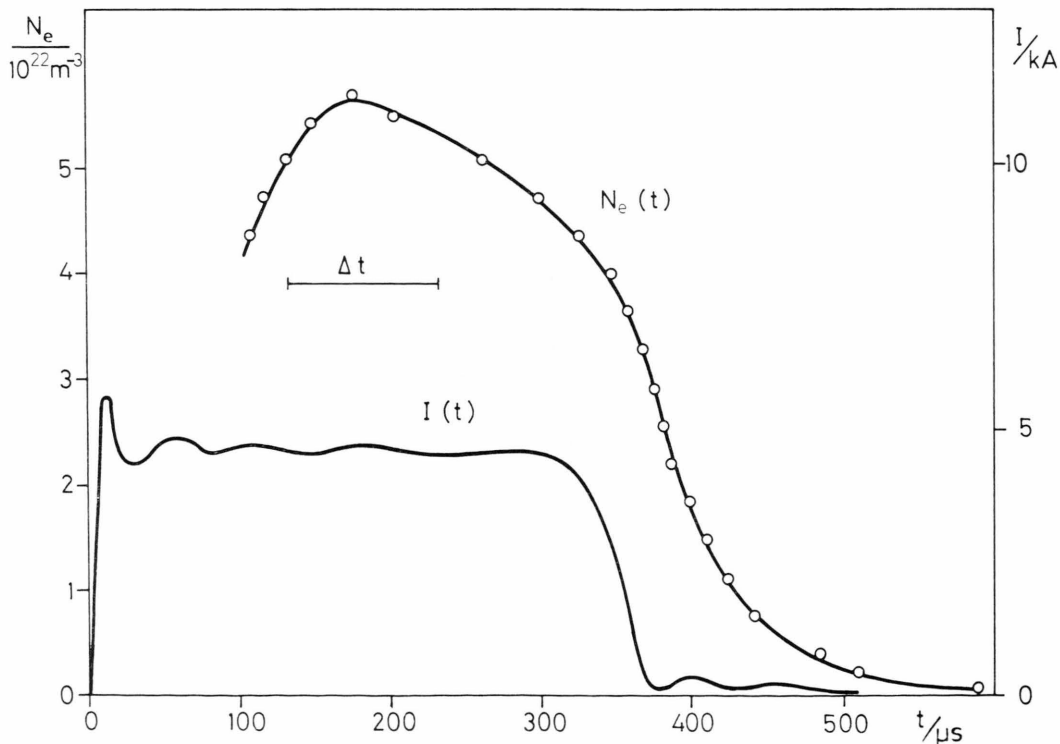

Fig. 4. Electron density and discharge current for typical discharge conditions ($U_0 = 14$ kV, $p_{He} = 2 \cdot 10^3$ Pa). Δt is the sample time interval.
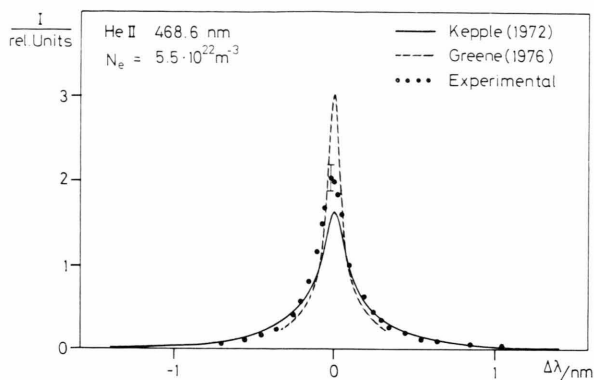
Fig. 5. Area normalized profiles of the Paschen-α line HeII 468.6 nm at $N_e = 5.5 \cdot 10^{22}$ m^{-3}.

scatter between independently measured line shapes. The total uncertainty of the electron density is less than 10%. It is essentially due to plasma irreproducibilities and to the density variation during the 100 μs sample time.

1. HeII 468.6 nm

In Fig. 5 the measured profile of the Paschen-α line is compared with theoretical profiles of Kepple [2] and of Greene [1]. All profiles are area normalized, after correcting the experimental profile for background intensity. The instrument function as well as Doppler broadening are neglected, since they amount to less than 10% of the measured line width. Obviously the experimental profile lies between the profiles of Kepple and Greene. This tendency is in qualitative agreement with the results obtained by other authors [6−9].

2. HeII 164.0 nm

Since the Balmer-α line is quite sensitive to self-absorption, the influence of optical depth on the measured line shape was experimentally checked. For this purpose several line profiles were measured at identical plasma parameters, but different plasma lengths. The length of the observed plasma zone could be varied by inserting a thin quartz rod along the discharge axis (Figure 1). The rod was mounted at the far end of the discharge tube. The measured relative line shape was found to be independent of the quartz rod position. Thus self absorption is

negligible and area normalization can be used to compare our measured line profiles with theoretical ones.

According to the small width of the Balmer-α line, Doppler and instrument broadening have to be taken into account. The instrument profile was determined by measuring sufficiently narrow CII lines emitted from discharges in CO_2. For slit widths of 10 μm, as used in this experiment, the instrument function turned out to be approximately Gaussian with a FWHM of 13 pm. The Doppler temperature was assumed to be sufficiently close to the electron temperature. This is a good approximation for our discharge conditions [18] and has been experimentally confirmed by Durand [19], who used a discharge similar to ours. For immediate comparison with experimental results the theoretical line profiles are convolved with both instrument function and Doppler profile. Background subtraction was not necessary.

Another, even more serious problem arises from the fine structure splitting of the Balmer-α line, which is neglected in the available theories. Since the separation of the two strongest fine structure components of the Balmer-α transition is 14 pm [20], this effect is of the same order of magnitude as the broadening mechanisms discussed above. The complete degeneracy of states with the same principal quantum number, which is usually a good approximation at high densities, is no longer justified for the parameters considered here. Therefore we have made a rather simple approach to include fine structure splitting.

Since Stark effect and fine structure of a quantum state n show opposite dependence on n, we take the n = 3 level as purely Stark broadened and the n = 2 level as being affected by fine structure splitting only. These assumptions allow the treatment of the Balmer-α line as a superposition of its different fine structure components, each of them individually Stark broadened according to the theory considered. In Fig. 6 the measured HeII 164.0 nm line profile is compared with several theoretically predicted profiles, which include instrument broadening, Doppler broadening and fine structure splitting in the way pointed out above. As can be seen from Fig. 6, the experimental profile is in good agreement with the results of Kepple [2] and Greene [4], at least in the line core. On the other hand, the earlier calculations of Greene [1] yield a slightly narrower profile,
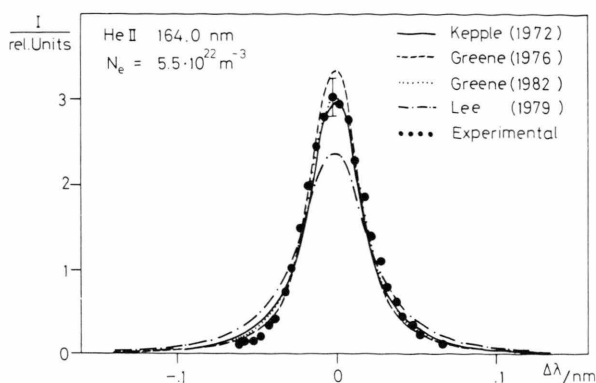
Fig. 6. Area normalized profiles of the Balmer-α line HeII 164.0 nm at $N_e = 5.5 \cdot 10^{22}$ m^{-3}. Theoretical profiles are corrected for fine structure splitting.

Fig. 9. Area normalized profiles of HeII 121.5 nm at $N_e = 5.5 \cdot 10^{22}$ m^{-3}. Absorption due to hydrogen impurities is suppressed by heating the discharge tube.
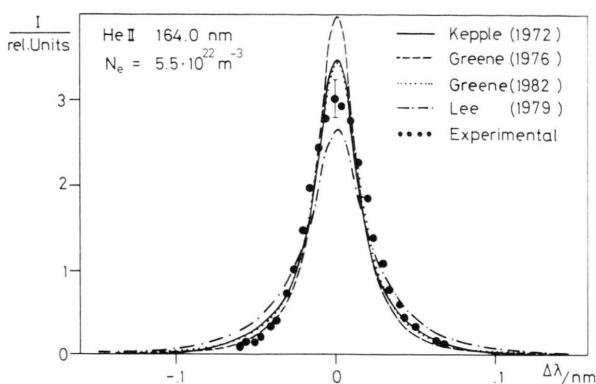

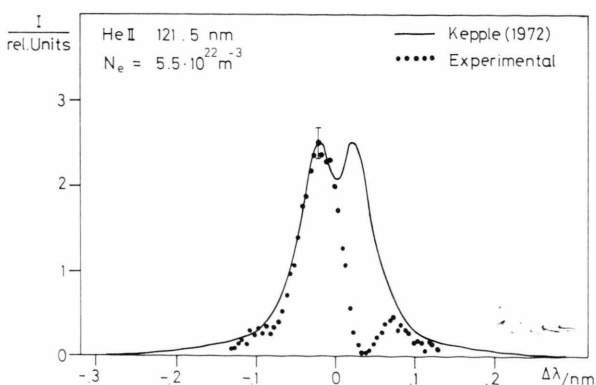
Fig. 7. Same as Fig. 6, but fine structure not included.

Fig. 8. Measured profile of the Balmer-β line HeII 121.5 nm with hydrogen Lyman-α absorption and theoretical profile normalized to equal peak intensity for comparison.
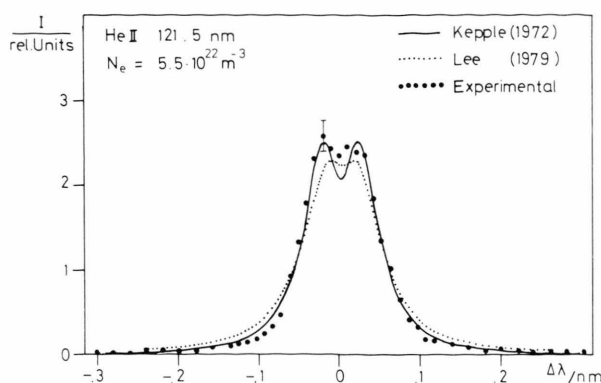
whereas the profile according to Lee [5] is much wider than the measured one. To illustrate the influence of fine structure, the corresponding profiles without fine structure are shown in Figure 7. The profiles turn out to be significantly narrower.

3. HeII 121.5 nm

Our first experimental profiles of the HeII 121.5 nm line were strongly asymmetric, the red peak of the expected double-peaked Stark profile being nearly suppressed, as shown in Figure 8. This was interpreted to be due to hydrogen Lyman-α reabsorption due to hydrogen impurities in cooler boundary layers. This effect has also been discussed earlier by van Zandt et al. [13], who measured widths and shifts of the HeII 121.5 nm line at higher densities. However, in our experiment the hydrogen impurities can be nearly removed by heating the discharge tube, as described in detail in Chapter I. In this way profiles of the HeII Balmer-β line were measured, essentially free of hydrogen Lyman-α reabsorption. In Fig. 9 the experimentally determined Balmer-β profile is compared with theoretical profiles of Kepple [2] and Lee [5]. Since the Balmer-β line is unaffected by self absorption, area normalization could be employed immediately. Theoretical profiles have been corrected for instrumental and Doppler broadening. Fine structure effects turned out to be negligible as compared to the resultant line width. In qualitative accordance with the results for the Balmer-α line, Lee's profile is found to be significantly wider in the near wings

than the measured profile. The profile according to Kepple is seen to fit quite well, except for the too pronounced central structure.

IV. Summary and Conclusion

Employing an improved plasma source of high purity and good reproducibility, Stark broadened HeII profiles of the Paschen-α, Balmer-α and Balmer-β line were measured at $N_e = 5.5 \cdot 10^{22}$ m^{-3} and $T_e = 3.8$ eV. The electron density was determined with an accuracy of better than 5% by means of a laser interferometer. At these plasma parameters even the Balmer-α line, which is most sensitive to self absorption, was found to be optically thin. Furthermore, due to the low impurity concentration, the Balmer-β profile was measured essentially free of hydrogen Lyman-α reabsorption. Thus reliable results were obtained in particular for the line core, which is of main importance for comparison with the different theories.

In case of the Paschen-α line HeII 468.6 nm calculations according to the modified impact theory of Kepple [2] yield wider profiles than the measurement, whereas the unified theory approach of Greene [1] predicts narrower line shapes. The major difference between these theories lies in the different treatment of the upper-lower state interference terms, which are not fully included in [2]. Ion-dynamic effects are neglected in both theories. However, as pointed out in [4], the additional broadening due to ion-radiator relative motion may probably explain the remaining discrepancies between Greene's calculations and our experimental results. The importance of ion-dynamic effects is supported by our results for the HeII Balmer lines. For the Balmer-α transition, a direct comparison between unified theory results with and without ion-dynamic effects [1, 4], respectively, and experimentally determined line shapes was performed.

The calculations of Greene [4], including ion-dynamics, were found to fit quite well with the experimental results, after taking fine structure splitting into account. In case of the Balmer-β line the discrepancies between our measurements and the calculations of Kepple, regarding the central line structure, might also be attributed to the neglect of ion-dynamics.

Balmer line shapes according to Lee [5] were found to be remarkably wider than the measured line profiles. This tendency is expected, since Lee's calculations agree with Kepple's treatment of the upper-lower state interference term, but additionally include ion-dynamics. In fact Lee's profiles agree with Kepple's results in the static limit [5]. However, the influence of upper-lower state interference on the line shape decreases with increasing Δn of the transition considered. This is qualitatively in agreement with the fact that the discrepancy between Lee's calculations and the measured line shape is smaller for the Balmer-β line than for the Balmer-α line.

The importance of both ion-dynamic effects as well as a complete treatment of the interference term in calculating Stark profiles has already been pointed out for hydrogen lines by Seidel [21], and we expect a similar influence for the HeII lines.

[1] R. L. Greene, Phys. Rev. A **14,** 1447 (1976).
[2] P. C. Kepple, Phys. Rev. A **6,** 1 (1972).
[3] H. R. Griem and K. Z. Shen, Phys. Rev. **122,** 1490 (1961).
[4] R. L. Greene, J. Phys. B.: Atom. Molec. Phys. **1982,** 1831.
[5] R. W. Lee, J. Phys. B.: Atom. Molec. Phys. **12,** No. 7 (1979).

[6] M. A. Bacon, A. J. Barnard, and F. L. Curzon, J. Quant. Spectroscop. Radiat. Transfer **18,** 399 (1977).
[7] H. Soltwisch and H. J. Kusch, Z. Naturforsch. **34 a,** 300 (1979).
[8] T. Oda and S. Kiriyama, J. Phys. Soc. Japan **49,** No. 1, 385 (1980).

[9] J. E. Bernard, F. L. Curzon, and A. J. Barnard, in: Spectral Line Shapes, ed. B. Wende, de Gruyter, Berlin 1981, pp. 153–164.

[10] L. A. Jones, J. R. Greig, T. Oda, and H. R. Griem, Phys. Rev. **4,** 833 (1971).

[11] H. Hessberg and W. Boetticher, Z. Naturforsch. **22 a,** 316 (1967).

[12] A. Eberhagen and R. Wunderlich, Z. Physik **232,** 1 (1970).

[13] J. R. Van Zandt, J. C. Adcock, and H. R. Griem, Phys. Rev. A **14,** 2126 (1976).

[14] C. C. Smith and D. D. Burgess, J. Phys. B.: Atom. Molec. Phys. **11,** No. 12 (1978).

[15] A. Piel and H. Richter, Z. Naturforsch. **38 a,** 37 (1983).

[16] D. E. T. F. Ashby and D. F. Jephcott, Appl. Phys. Lett. **3,** 13 (1963).

[17] R. Mewe, Brit. J. Appl. Phys. **18,** 107 (1967).

[18] W. Finkelnburg and H. Maecker, in: Handbuch der Physik, Vol. 22, ed. S. Flügge, Springer-Verlag, Berlin 1956, pp. 254–444.

[19] J. Durand, Z. Naturforsch. **18 a,** 281 (1963).

[20] C. Candler, Atomic Spectra, Hilger and Watts Ltd., London 1964.

[21] J. Seidel, in: Spectral Line Shapes, ed. B. Wende, de Gruyter, Berlin 1981, pp. 3–40.